A Continuous 55 Million Year Record of Transient Mantle Plume Activity Beneath Iceland

Ross Parnell-Turner[1], Nicky White[1], Tim Henstock[2], Bramley Murton[3], John Maclennan[1] & Stephen Jones[4]

[1] *Department of Earth Sciences, University of Cambridge, Cambridge, CB3 0EZ, UK*

[2] *National Oceanography Centre Southampton, University of Southampton, Southampton SO17 1BJ, UK*

[3] *National Oceanography Centre, European Way, Southampton, SO14 3ZH, UK*

[4] *School of Geography, Earth and Environmental Sciences, University of Birmingham, B15 2TT, UK*

In the North Atlantic Ocean, the mid-oceanic ridge transects the Icelandic mantle plume, providing an important window into the temporal evolution of this major convective upwelling[1–3]. It is generally accepted that different periodicities of transient behavior are indirectly recorded within the fabric of the oceanic floor south of Iceland[4–7]. Despite its significance, the detailed structure of this region is poorly known. To address this shortcoming, we present long seismic reflection profiles that traverse the entire oceanic basin between northwest Europe and Greenland. A diachronous pattern of V-shaped ridges is clearly imaged beneath a thickening blanket of sediment, revealing a complete record of transient convective behavior that can be traced continuously back to ∼55 Myrs— the longest record of its kind. Periodicity increases from ∼3 to ∼8 Myr with clear evidence for minor, but systematic, asymmetric crustal accretion. The amplitudes of these V-shaped ridges grow with time and reflect small (e.g. 5–30°C) fluctuations of mantle potential temperature that are consistent with episodic generation of hot solitary waves at a thermal boundary layer deep within the mantle[8]. Our continuous record of convective activity has implications for the fluid dynamics of mantle processes, as well as significant paleoceanographic and geomorphic consequences.

Spatial and temporal patterns of convective circulation beneath lithospheric plates cause regional elevation changes at the Earth's surface which have important— but poorly understood— implications for landscape development on geologic timescales. Since the Rayleigh number of convecting mantle is 10^6–10^8, this circulation is expected to be transient, varying on timescales of 1–100 Myr and on length scales of 100s–1000s of kilometers[3,9]. A global network of mid-oceanic ridges provides a useful means of estimating the temperature of underlying asthenosphere[10,11]. At spreading mid-oceanic ridges, accretion of oceanic crust is sensitive to small temperature fluctuations that change the thickness of newly formed crust by kilometers[2]. In the North Atlantic ocean, the Reykjanes Ridge bisects the Icelandic plume, a hot convective upwelling with a radius of at least 1200 km[12].

Within the region influenced by this plume, average thickness of oceanic crust increases from 7 to 14 km and the seabed is anomalously shallow by up to 2 km. Both observations are consistent with an average temperature anomaly of 150°C [2]. Several different timescales of transient behavior are sampled by the mid-oceanic ridge's interaction with this plume. On the shortest timescale, the most obvious and best-known features are diachronous V-shaped ridges (VSRs) that are visible on either side of the ridge axis where sedimentary cover is minimal (Figure 1). These VSRs probably reflect minor changes in the thickness and composition of oceanic crust and are generated when hotter than average parcels of plume material travel radially away from the plume's conduit[13,14]. On a much longer timescale, there is a transition from smooth crust without fracture zones, accreted over hotter asthenosphere, to rough crust with fracture zones, accreted over colder asthenosphere. This observation suggests that the plume's planform has changed through time. Today, the plume's influence extends at least as far south as the intersection between the mid-oceanic ridge and the Bight Fracture Zone at 57°N and 33°W [2,5]. Despite their importance in providing otherwise inaccessible insights into convective processes, the structure and extent of these VSRs are poorly known and their origin is debated[15,16]. It is especially unclear how many VSRs exist and how far back in time their history can be traced.

To address these general issues, we acquired two regional (>1200 km) seismic reflection profiles that traverse the entire oceanic basin south of Iceland (Figure 1). Crucially, both profiles provide conjugate images of the Iceland and Irminger basins since each one of them is oriented parallel to plate spreading flowlines[17]. Acquisition and processing details are provided in the Methods Summary. We have two significant findings. First, we have mapped the sediment-basement interface, which demonstrates that VSR activity can be continuously traced back to 55 Myr. Secondly, this activity has been used to build a detailed chronology of asthenospheric potential temperature, T_P. This continuous record provides a reference frame for analyzing relationships between plume activity and other geologic observations.

The northern profile resolves the detailed structure of this oceanic basin (Figure 2a). Away from a prominent mid-oceanic ridge, the top of oceanic crust is clearly imaged beneath layered sediments, which thicken in either direction. A sediment-basement interface can easily be traced despite being cut by minor faults (Figure 2a). The sedimentary pile is dominated by contourite drift deposits that record the history of deep-water overflow across the Greenland-Iceland-Scotland ridge. For example, Eirik drift records 7 Myr of overflow through the Denmark Straits and is visible at the northwestern end of the profile. This overflow caused incision of older contourite deposits northwest of the mid-oceanic ridge. The sediment-basement interface is deformed into a series of prominent ridges and troughs that are imaged out to $\sim$500 km on either side of the mid-oceanic ridge. These long wavelength features (i.e. VSRs) are 20–40 km wide with amplitudes of up to 1 km. They also correlate with small free-air gravity anomalies whose significance was not previously recognized (Figure 2c,d). Detailed interpretation shows that these ridges and troughs are broken up, but not defined, by normal faulting (Figure 2e,f).

Average crustal thickness along the Reykjanes Ridge is primarily controlled by asthenospheric temperature within the plume head[13]. Smallwood et al.[17] demonstrated that V-shaped ridges and troughs are maintained by minor changes in oceanic crustal thickness, which in turn are generated by temperature fluctuations within the plume. Changes in the composition of basaltic rocks and in the geometry of active faults along the Reykjanes Ridge suggest that these temperature fluctuations are $\pm 25^{\circ}$C[13,14,18]. Here, we exploit residual depth anomalies as a proxy for tracking crustal thickness and asthenospheric temperature fluctuations (Figure 3a). Residual depth is the water-loaded depth to oceanic crust that has been corrected for sediment loading, plate age and present-day dynamic support[6]. South of Iceland, residual depth varies by ± 400 m and is controlled by changes in crustal thickness. If crust is generated at the mid-oceanic ridge by isentropic decompression of anhydrous mantle[11,13], T_p can be estimated from residual depth measurements using

$$T_p \approx 16 \left[t_c + \left(\frac{\rho_a - \rho_w}{\rho_a - \rho_c} \right) d_r \right] + 1200 \tag{1}$$

where $t_c = 8.4$ km is a reference crustal thickness[17], d_r is residual depth, $\rho_a = 3.2$ Mg m^{-3} is density of asthenospheric mantle, $\rho_c = 2.8$ Mg m^{-3} is density of oceanic crust, and $\rho_w = 1$ Mg m^{-3} is density of seawater[6,13]. We have projected our T_p estimates into age-distance space and combined them with satellite gravity observations (Figure 3b). There is excellent agreement between these estimates and free-air gravity anomalies on young, smooth oceanic crust ($<$20 Myr). On the oldest crust, VSRs are also visible and correlate with weak but linear gravity anomalies, despite variable thicknesses of sedimentary cover (Figure 1). Parkin and White[19] demonstrated that some of the oldest VSRs are manifest by resolvable crustal thickness differences of ± 1 km. At radial distances of $>$500 km from the plume center, symmetric lobes of cooler oceanic crust are intersected by the southern profile between 20 and 35 Myr (Figure 3b). Within these highly faulted lobes, coherent VSRs are not clearly observed and legacy seismic refraction data suggest that the crust is only 6.1 km thick [5,20].

VSRs are not perfectly symmetric about the Reykjanes Ridge. For example, an old and prominent VSR occurs at 33 Myrs on eastern side of the northern profile (Figure 3a). On the western side of the same profile, this VSR occurs at 35 Myrs, which corresponds to a cumulative offset of 20 km. Over the last 30 Myrs, a systematic pattern of increasing offset is consistent with a history of asymmetric crustal accretion documented using magnetic anomaly profiles located closer to Iceland[15,16]. At distances of $<$250 km from the ridge axis, estimates of asymmetry made from magnetic anomalies and VSRs agree (Figure 3c). Increasing asymmetry corresponds to a series of well-known eastward ridge jumps on Iceland which reflect the fact that the mid-oceanic ridge gradually drifts westward with respect to the plume center, periodically relocating itself at the center of the plume[21]. VSR asymmetry between 300 and 500 km corresponds to a much older westward switching in seafloor spreading from the now-extinct Aegir Ridge to the active Kolbeinsey Ridge located north of Iceland[22,23].

This growth and decay of asymmetry enables us to synchronize VSR chronology on either side of the Reykjanes Ridge (Figure 3d). The resultant match between eastern and western portions of our profile implies that the VSRs themselves are likely to have been generated by temperature fluctuations deep within the structure of the plume[7,14,15]. Growth and decay of asymmetric spreading appears to correlate with plume activity. In the North Atlantic Ocean, the mid-oceanic ridge drifts northwestward with respect to the center of the plume. Our results suggest that the cumulative amount of drift grows when the plume is more quiescent (compare Figures 3c and d). An increase in plume activity increases the distal radial force that acts to inhibit plate spreading and encourages the mid-oceanic ridge to relocate back to the plume center. If elevation at the plume center increases by 200 m, the distal radial force can increase by 2×10^8 N m^{-1}.

Between 55 and 35 Myrs, small (~ 5–$10°$C) fluctuations of plume temperature have a periodicity of $\sim$ 3 Myrs. These fluctuations are superimposed upon a rapidly cooling temperature structure that is also manifest by a northward shift in the transition from smooth to rough crust. Both observations are consistent with dramatic plume shrinkage [19]. After 35 Myrs, the radius of the convective planform rapidly regrew from 400 to at least 1200 km. This growth was accompanied by large ($\sim$ 25–$30°$C) fluctuations of plume temperature that have a irregular periodicity of up to 8 Myrs (Figure 3d). This changing periodicity is probably caused by boundary layer perturbations within the convecting mantle [4,5,19,24]. Scaling analysis suggests that VSR activity is compatible with perturbations which form either at the 670 km mantle discontinuity or at the core-mantle boundary (Supplementary Information).

Using values from Supplementary Table 1, the geometry of the youngest VSR confirms that the present-day buoyancy flux of the plume is $B = 18 \pm 7$ Mg s^{-1} if plume material flows radially away from the plume center within an asthenospheric layer that is 125 $\pm$ 25 km thick with an excess temperature of $\Delta T = 150 \pm 50°$C [6,7]. Independent values of B can be obtained by exploiting two separate observations. First, the changing boundary between smooth and rough crust, d, is controlled by a combination of plate spreading rate, u, and B where

$$B = \pi u d^2 \rho_m \alpha \Delta T \tag{2}$$

which yields B = 26 $\pm$ 9 Mg s^{-1} for the last 2 Myrs. Secondly, the present-day planform of the plume swell constrains its excess volume [25]. If a plume radius of 1200 ± 100 km grew over the last 25–35 Myrs, B = 17

$\pm$ 5 Mg s^{-1}. These three independent estimates of buoyancy flux are consistently large, indicating that the Iceland plume is one of the biggest convective upwellings on Earth. In contrast, the Hawaiian plume has a buoyancy flux of 8.7 Mg s^{-1} (ref. 26).

Our seismic reflection interpretations suggest that buoyancy flux has changed through time. Within the Irminger and Iceland basins, the oldest VSRs have weak linear gravity anomalies that yield B = 73 $\pm$ 15 Mg s^{-1} and 66 $\pm$ 14 Mg s^{-1}, respectively. These values are consistent with the oldest smooth lobes of crust that extend at least 1400 km away from the center of the plume, implying that $B \geq 70$ Mg s^{-1} (Figure 3b).

Finally, our observations help to bound the dimensions of solitary waves that are generated at putative thermal boundary layers and travel up deformable conduits of plumes (Figure 4)[8]. In the plate spreading direction, the youngest VSRs are 25–30 km wide whereas older ones are 15–20 km wide. The youngest VSR is $\sim$730 km from the plume center and has a width x = 25 $\pm$3 km. Assuming a present-day plume flux of $\sim$18 $\pm$ 4 Mg s^{-1}, the along-axis width, ΔR, is predicted to be 244 $\pm$ 44 km. This value is consistent with a 250 km long segment of increased volcanism and reduced seismicity along the mid-oceanic ridge crest near 60°N[18].

In summary, we present observations which document a continuous record of transient behaviour of the Icelandic plume between 55 Myrs and the present day. Transient thermal anomalies occur every 3–8 Myr and are generated by boundary layer instabilities. Present-day buoyancy flux of the Iceland plume indicates that it is one of the larger convective upwelling on Earth. Fluctuating dynamic support during the Cenozoic Era provides a general mechanism for proposed changes in deepwater oceanic circulation[14], for sedimentary drift accumulation[27], and for the carving of ancient ephemeral landscapes[28]. Establishing these connections between convective chronologies and surface observations will yield novel insights into the coupled nature of Earth's deep and shallow realms.

Methods Summary

Seismic data acquisition and processing. Seismic profiles were acquired onboard the RRS *James Cook* during July–August 2010 by the Universities of Cambridge, Southampton and Birmingham. This cruise, JC50, was financially supported by the Natural Environmental Research Council. Acoustic energy was generated using a single generator-injector airgun with a total volume of 5.82 litres (generator pulse = 4.1 litres, injector pulse = 1.72 litres) and a frequency bandwidth of 10–400 Hz. The airgun was towed at a depth of 5.5 m behind the vessel, which steamed at $\sim$9.3 km hr^{-1}. This airgun was primed with compressed air (20.7 MPa) and fired every 15 s ($\sim$40 m). Reflected acoustic energy was recorded on a 1600 m-long streamer towed at 7 m depth. This streamer consisted of 132 groups of hydrophones located every 12.5 m. Distance from the airgun to the first group (i.e. near-trace offset) was 163 m. The digital sampling interval of recorded signals was 1 ms. During the survey, impulses of acoustic energy are transmitted and reflected at discontinuities within the Earth, where changes in acoustic impedance are generated by density and velocity contrasts. The geometry of this survey was designed to repeatedly record signals every 6.25 m along the profile. This redundancy improves signal to noise since reflections from different shotpoint–receiver pairs can be stacked together. Before stacking, acoustic velocity is carefully picked as a function of depth to correct for the travel-time delay (that is, normal move-out) of different raypaths within a single common mid-point (CMP) gather. Here, velocity functions were hand-picked every 100 CMPs (i.e. every 625 m). The resultant 21-fold stacked image has a vertical and horizontal resolution of 10–20 m. Signal processing techniques also included application of a 12 Hz high-pass filter with a roll-off of 24 dB per octave, and a post-stack Stolt migration with a constant acoustic velocity of 1500 m s^{-1}.

References

1. Vogt, P. R. Asthenosphere motion recorded by the ocean floor south of Iceland. *Earth Planet. Sci. Lett.* **13**, 153–160 (1971).

2. White, R. S. Rift-plume interaction in the North Atlantic. *Philos. Trans. R. Soc. Lond. A* **355**, 319–339 (1997).

3. Schubert, G., Turcotte, D. L. & Olson, P. *Mantle Convection in the Earth and Planets* (Cambridge University Press, 2001).

4. Ito, G. Reykjanes 'V'-shaped ridges originating from a pulsing and dehydrating mantle plume. *Nature* **411**, 681–684 (2001).

5. Jones, S. M., White, N. J. & Maclennan, J. V-shaped ridges around Iceland: Implications for spatial and temporal patterns of mantle convection. *Geochem. Geophys. Geosyst.* **3**, 1059 (2002).

6. Poore, H. R., White, N. J. & Jones, S. M. A Neogene chronology of Iceland plume activity from V-shaped ridges. *Earth Planet. Sci. Lett.* **283**, 1–13 (2009).

7. Jones, S. M. *et al.* A joint geochemical-geophysical record of time-dependent mantle convection south of Iceland. *Earth Planet. Sci. Lett.* **386**, 86–97 (2014).

8. Schubert, G., Olson, P., Anderson, C. & Goldman, P. Solitary waves in mantle plumes. *J. Geophys. Res.* **94**, 9523–9532 (1989).

9. Loper, D. E. & Stacey, F. D. The dynamical and thermal structure of deep mantle plumes. *Phys. Earth Planet. Inter.* **33**, 304–317 (1983).

10. Klein, E. M. & Langmuir, C. H. Global correlations of ocean ridge basalt chemistry with axial depth and crustal thickness. *J. Geophys. Res.* **92**, 8089–8115 (1987).

11. McKenzie, D. P. & Bickle, M. J. The Volume and Composition of Melt Generated by Extension of the Lithosphere. *J. Petrol.* **29**, 625–679 (1988).

12. Rickers, F., Fichtner, A. & Trampert, J. The Iceland Jan Mayen plume system and its impact on mantle dynamics in the North Atlantic region: Evidence from full-waveform inversion. *Earth Planet. Sci. Lett.* **367**, 39–51 (2013).

13. White, R. S., Bown, J. & Smallwood, J. R. The temperature of the Iceland plume and origin of outward-propagating V-shaped ridges. *J. Geol. Soc.* **152**, 1039–1045 (1995).

14. Poore, H. R., White, N. J. & Maclennan, J. Ocean circulation and mantle melting controlled by radial flow of hot pulses in the Iceland plume. *Nature Geosci.* **4**, 558–561 (2011).

15. Hey, R., Martinez, F., Höskuldsson, Á. & Benediktsdóttir, Á. Propagating rift model for the V-shaped ridges south of Iceland. *Geochem. Geophys. Geosyst.* **11**, Q03011 (2010).

16. Benediktsdóttir, Á., Hey, R., Martinez, F. & Höskuldsson, Á. Detailed tectonic evolution of the Reykjanes Ridge during the past 15 Ma. *Geochem. Geophys. Geosyst.* **13**, Q02008 (2012).

17. Smallwood, J. R. & White, R. S. Crustal accretion at the Reykjanes Ridge. *J. Geophys. Res.* **103**, 5185–5201 (1998).

18. Parnell-Turner, R. E. *et al.* Crustal manifestations of a hot transient pulse at 60°N beneath the Mid-Atlantic Ridge. *Earth Planet. Sci. Lett.* **363**, 109–120 (2013).

19. Parkin, C. J. & White, R. S. Influence of the Iceland mantle plume on oceanic crust generation in the North Atlantic. *Geophys. J. Int.* **173**, 168–188 (2008).

20. Whitmarsh, R. B. Seismic anisotropy of the uppermost mantle absent beneath the east flank of the Reykjanes Ridge. *Bull. Seismol. Soc. Am.* **61**, 1351–1368 (1971).

21. Hardarson, B., Godfrey Fitton, J., Ellam, R. M. & Pringle, M. S. Rift relocation – a geochemical and geochronological investigation of a palaeo-rift in northwest Iceland. *Earth Planet. Sci. Lett.* **153**, 181–196 (1997).

22. Jung, W.-Y. & Vogt, P. R. A gravity and magnetic anomaly study of the extinct Aegir Ridge, Norwegian Sea. *J. Geophys. Res.* **102**, 5065–5089 (1997).

23. Smallwood, J. R. & White, R. S. Ridge-plume interaction in the North Atlantic and its influence on continental breakup and seafloor spreading. *Geol. Soc. Spec. Pub.* **197**, 15–37 (2002).

24. Olson, P., Schubert, G. & Anderson, C. Plume formation in the D″-layer and the roughness of the core–mantle boundary. *Nature* **327**, 409–413 (1987).

25. Crosby, A. G. & McKenzie, D. P. An analysis of young ocean depth, gravity and global residual topography. *Geophys. J. Int.* **178**, 1198–1219 (2009).

26. Sleep, N. H. Hotspots and Mantle Plumes: Some Phenomenology. *J. Geophys. Res.* **95**, 6715–6736 (1990).

27. Wold, C. N. Cenozoic sediment accumulation on drifts in the northern North Atlantic. *Paleoceanography* **9**, 917–941 (1994).

28. Hartley, R. A., Roberts, G. G., White, N. J. & Richardson, C. Transient convective uplift of an ancient buried landscape. *Nature Geosci.* **4**, 562–565 (2011).

29. Sandwell, D. T. & Smith, W. H. F. Global marine gravity from retracked Geosat and ERS-1 altimetry: Ridge segmentation versus spreading rate. *J. Geophys. Res.* **114**, B01411 (2009).

30. Shorttle, O., Maclennan, J. & Jones, S. M. Control of the symmetry of plume-ridge interaction by spreading ridge geometry. *Geochem. Geophys. Geosyst.* **11**, Q0AC05 (2010).

Supplementary Information is linked to the online version of the paper at www.nature.com/nature

Acknowledgments This research is supported by NERC Grant NE/G007632/1 and by the Girdler Fund, University of Cambridge. We thank the Master, crew and technicians of RRS *James Cook* Cruise JC50 for their dedicated professionalism. We are grateful to J. Rudge for assisting with the boundary layer scaling analysis. Earth Sciences contribution number XXXX.

Author Contributions This project was conceived and managed by N.W. and co-authors. R.P-T. processed and interpreted seismic data with guidance from N.W. and T.H. The paper was written by R.P-T. and N.W. with contributions from co-authors.

Author Information Reprints and permissions information is available at www.nature.com/reprints. The authors declare that they have no competing financial interests. Correspondence and requests for material should be addressed to N.W. and R.P-T. (email: njw10@cam.ac.uk, rep52@cam.ac.uk).

1 Figure Captions

Figure 1: **Location of seismic experiment.** **a**, Bathymetric map showing location of seismic reflection profiles. Emboldened portion of profile 2 is shown in Figure 2. Red line = plate-spreading axis along Reykjanes Ridge. **b**, Map of free-air gravity anomalies filtered to remove wavelengths $>$250 km[29]. Red/blue circles at A = ridge/trough crustal thicknesses[17]; blue circle at B = crustal thickness from vintage seismic refraction experiment[20]; blue line at C = crustal thickness profile[19].

Figure 2: **Interpreted seismic images**. **a**, Profile 2 (Figure 1). Red line = free-air gravity anomaly[29]. **b**, Geologic interpretation. Solid lines = seabed and sediment-basement interface; yellow shading = sedimentary cover; dashed line = seabed multiple; red circles/lines = sets of VSRs; blue circles = intervening V-shaped troughs; vertical lines = locus of azimuthal changes along flowline. **c**, Young VSR ($\sim$12 Myr) and associated gravity anomalies. **e**, Geologic interpretation. Solid line = normally faulted sediment-basement interface; yellow shading = plastered contourite drifts. **d**, Structure of three older VSRs (35–40 Myr) and associated free-air gravity anomalies. **f**, Geologic interpretation. VSRs have steeper flanks facing toward mid-oceanic ridge.

Figure 3: **Analysis of VSR chronology and asymmetric crustal accretion.** **a**, Line = water-loaded basement depth on astronomical timescale[5]; gray line = mirror image; dashed lines = best-fitting relationships ($d = 580 + 430a^{1/2}$ and $d = 770 + 360a^{1/2}$ for western/eastern portions; d = depth; a = age); red circles/lines = VSRs (Figure 2); red/blue circles = crustal thicknesses[17,20]. **b**, Gravity anomaly as function of age and distance from plume center (63.95°N, 17.4°W)[30]. Lines = calculated T_p; red/blue circles = crust-derived T_P[17]; dashed/dotted lines = smooth-rough transition from magnetic/gravity picks[6]; blue dots = V-shaped troughs. **c**, Asymmetry of crustal accretion. Circles = asymmetry from magnetic picks[5,15]; red circles = VSR-derived asymmetry; line = best-fitting curve; bars = ridge-jump episodes[23]. E/W = jump direction; S-NVZ = Snaefellsnes-Húnafloí paleo-rift toward Northern Volcanic Zone. **d**, Residual depth and T_p as function of time adjusted to plume center. Black/gray lines = eastern/western portions of profile 2 corrected using **c**; red circles/lines = VSRs; red/blue circles = cruts-derived T_p[17,20]; blue band = T_p from wide-angle data[19].

Figure 4: **Cut-away cartoon showing plume geometry**. Red body = idealized plume spreading outward beneath lithosphere; darker patches = periodic blobs of hotter than average plume material flowing outward at $\sim$40 cm/yr; gray block = cooling/thickening lithosphere; red ribs = VSRs generated by plate spreading over plume; cut-away yellow prism = melting region beneath which hot annuli pass; red arrows indicate flow; l = length of solitary wave. Inset: relationship between thickened crust beneath VSR and underlying temperature structure. Gray band = crust where x is width of VSR parallel to flowline and ΔR is width of VSR along axis; cut-away yellow prism = melting region; red base = top of asthenosphere.

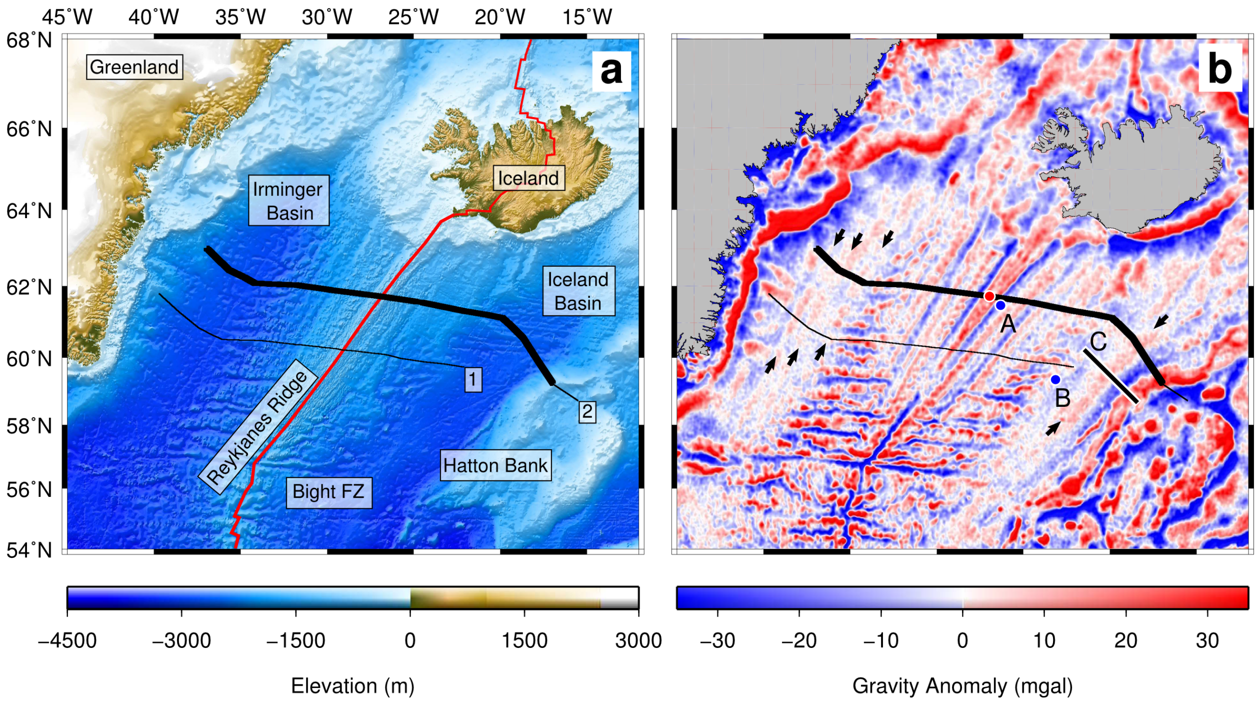

45˚W
40˚W
35˚W
30˚W
25˚W
20˚W
15˚W
68˚N
66˚N
64˚N
62˚N
60˚N
58˚N
56˚N
54˚N
a
Greenland
Irminger Basin
Iceland
Iceland Basin
Reykjanes Ridge
Bight FZ
Hatton Bank
1
2
b
A
B
C
–4500
–3000
–1500
0
1500
3000
Elevation (m)
–30
–20
–10
0
10
20
30
Gravity Anomaly (mgal)

Figure 1

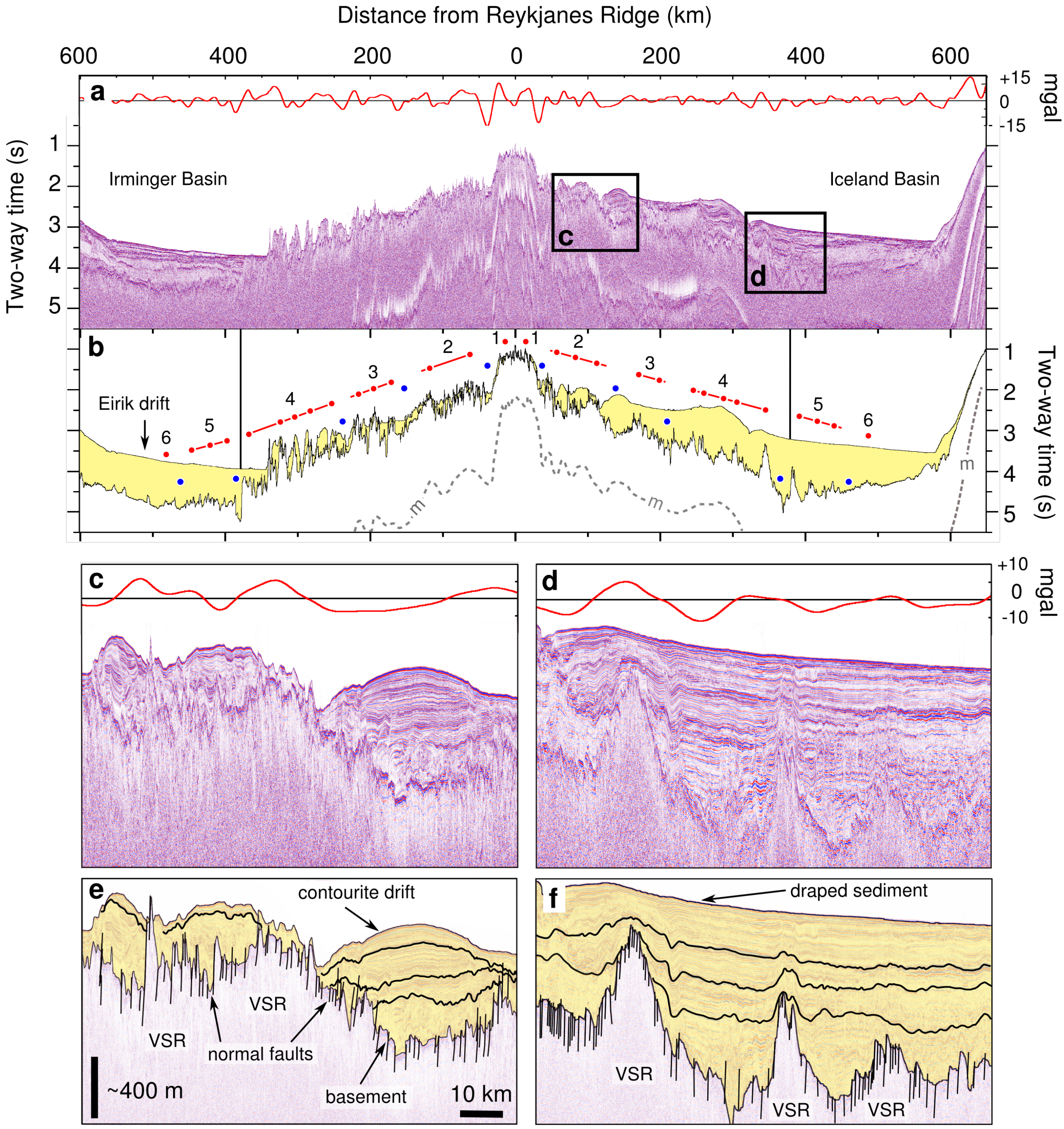

Distance from Reykjanes Ridge (km)
600
400
200
0
200
400
600
a
+15
0
-15
mgal
Two-way time (s)
1
2
3
4
5
Irminger Basin
Iceland Basin
c
d
b
Eirik drift
6
5
4
3
2
1
1
2
3
4
5
6
m
m
m
Two-way time (s)
c
d
+10
0
-10
mgal
e
contourite drift
VSR
VSR
normal faults
basement
~400 m
10 km
f
draped sediment
VSR
VSR
VSR

Figure 2

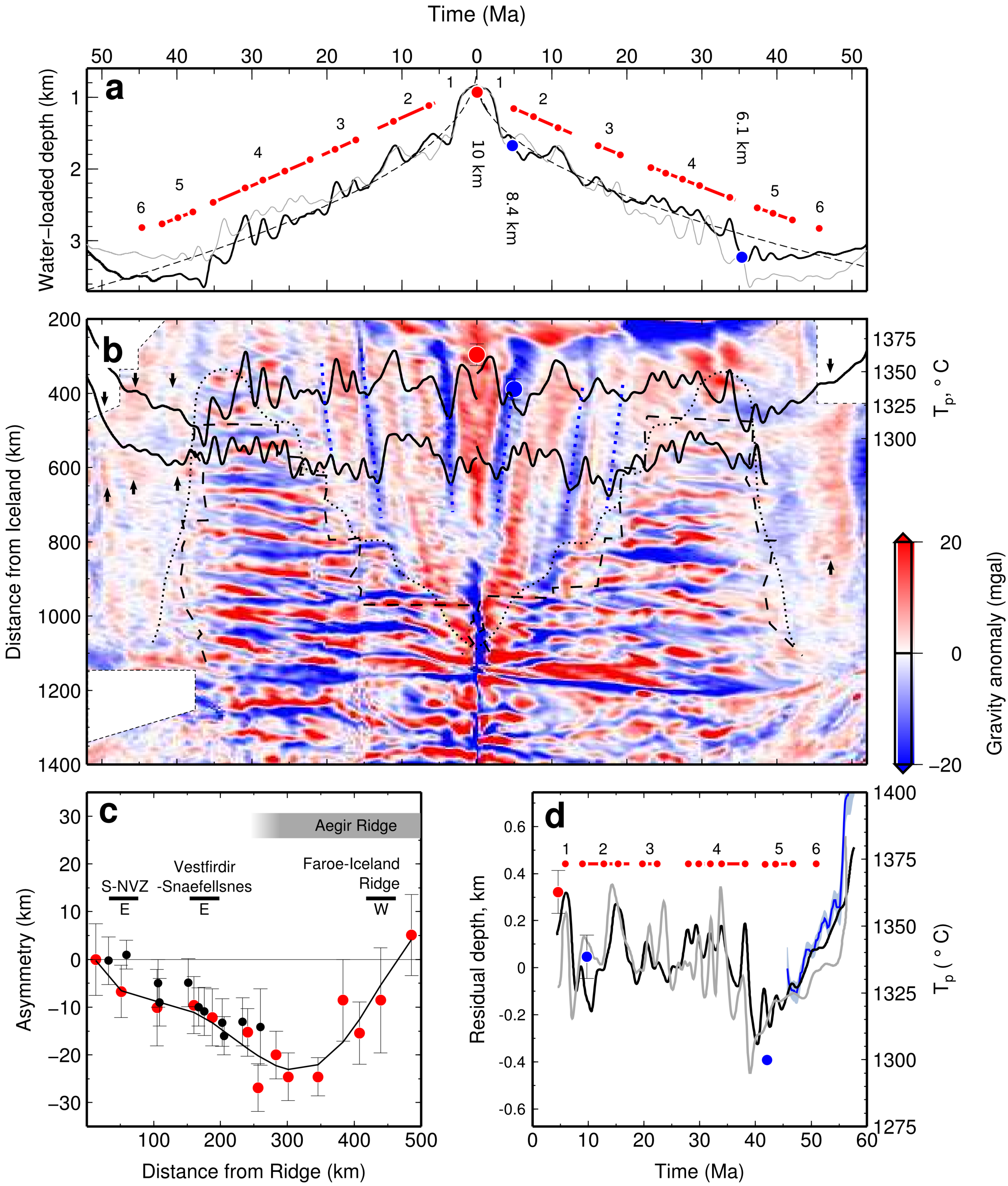

Time (Ma)
50 40 30 20 10 0 10 20 30 40 50
a
Water–loaded depth (km)
1 2 3
1 2 3 4 5 6
10 km
8.4 km
6.1 km
b
Distance from Iceland (km)
200 400 600 800 1000 1200 1400
1375 1350 1325 1300
T_p, °C
20 0 −20
Gravity anomaly (mgal)
c
Asymmetry (km)
30 20 10 0 −10 −20 −30
Aegir Ridge
S-NVZ
E
Vestfirdir
-Snaefellsnes
E
Faroe-Iceland
Ridge
W
100 200 300 400 500
Distance from Ridge (km)
d
Residual depth, km
0.6 0.4 0.2 0 -0.2 -0.4 -0.6
1 2 3 4 5 6
1400 1375 1350 1325 1300 1275
T_p (°C)
0 10 20 30 40 50 60
Time (Ma)

Figure 3

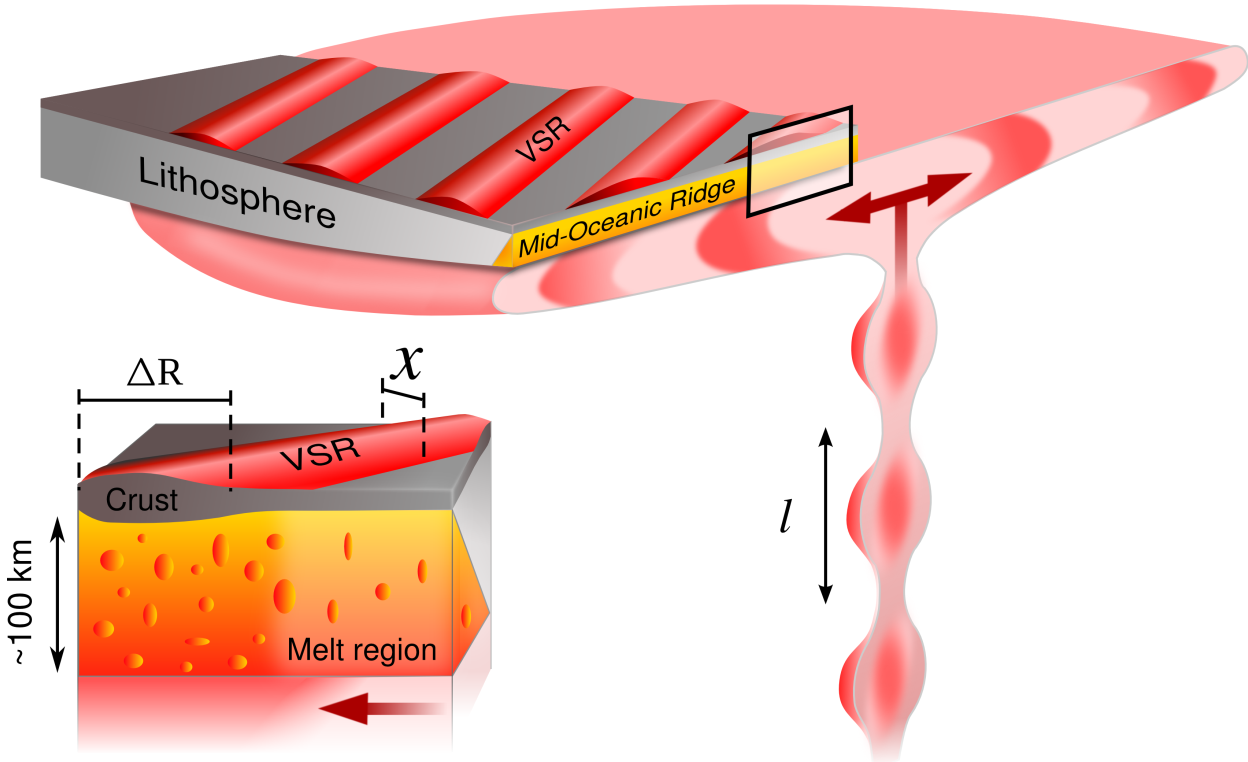
Lithosphere
VSR
Mid-Oceanic Ridge
ΔR
x
VSR
Crust
~100 km
Melt region
l

Figure 4